Journal of Solid State Chemistry 183 (2010) 2818–2825

Contents lists available at ScienceDirect

Journal of Solid State Chemistry

journal homepage: www.elsevier.com/locate/jssc

Full potential study of the elastic, electronic, and optical properties of spinels $MgIn_2S_4$ and $CdIn_2S_4$ under pressure effect

F. Semari [a], R. Khenata [b,c], M. Rabah [a], A. Bouhemadou [c,d], S. Bin Omran [c], Ali H. Reshak [e,f,*], D. Rached [a]

[a] Laboratoire des Matériaux Magnétiques, Département de Physique, Faculté des Sciences, Université Djillali Liabes de Sidi Bel Abbès, Sidi Bel Abbès 22000, Algeria
[b] Laboratoire de Physique Quantique et de Modélisation Mathématique (LPQ3M), Département de Technologie, Université de Mascara, Mascara 29000, Algeria
[c] Depatment of Physics and Astronomy, King Saud University, PO Box 2455, Riyadh 11451, Saudi Arabia
[d] Laboratory for Developing New Materials and their Characterization, Faculty of Science, University of Setif, 19000 Setif, Algeria
[e] Institute of Physical Biology, South Bohemia University, Nove Hrady 373 33, Czech Republic
[f] School of Microelectronic Engineering, University Malaysia Perlis (UniMAP), Block A, Kompleks Pusat Pengajian, 02600 Arau Jejawi, Perlis, Malaysia

ARTICLE INFO

Article history:
Received 13 June 2010
Received in revised form
2 September 2010
Accepted 19 September 2010
Available online 25 September 2010

Keywords:
FP-APW+lo
Spinel
Electronic structure
Elastic properties
Optical properties
Pressure effect

ABSTRACT

The structural, elastic, electronic, and optical properties of cubic spinel $MgIn_2S_4$ and $CdIn_2S_4$ compounds have been calculated using a full relativistic version of the full-potential linearized-augmented plane wave with the mixed basis FP/APW+lo method. The exchange and correlation potential is treated by the generalized-gradient approximation (GGA). Moreover, the Engel–Vosko GGA formalism is also applied to optimize the corresponding potential for band structure calculations. The ground state properties, including the lattice constants, the internal parameter, the bulk modulus, and the pressure derivative of the bulk modulus are in reasonable agreement with the available data. Using the total energy-strain technique, we have determined the full set of first-order elastic constants C_{ij} and their pressure dependence, which have not been calculated or measured yet. The shear modulus, Young's modulus, and Poisson's ratio are calculated for polycrystalline XIn_2S_4 aggregates. The Debye temperature is estimated from the average sound velocity. Electronic band structures show a direct band gap (Γ–Γ) for $MgIn_2S_4$ and an indirect band gap (K–Γ) for $CdIn_2S_4$. The calculated band gaps with EVGGA show a significant improvement over the GGA. The optical constants, including the dielectric function $\varepsilon(\omega)$, the refractive index $n(\omega)$, the reflectivity $R(\omega)$, and the energy loss function $L(\omega)$ were calculated for radiation up to 30 eV.

1. Introduction

The behavior of materials under compression based on calculations or measurements has become quite interesting in the last few years as it provides an insight into the nature of solid state theories and determines the values of fundamental parameters [1].

Elastic properties of a solid are important because they are closely related to various fundamental solid-state phenomena such as interatomic bonding, equation of state, and phonon spectra. Most importantly, knowledge of elastic constants is essential for many practical applications related to the mechanical properties of a solid: load deflection, thermoelastic stress, internal strain, sound velocities, and fracture toughness. Hence, it is always desirable to have general idea about the elastic moduli of material before its synthesis and its characterization, in order to tailor its properties.

The ternary semiconductor materials have recently attracted attentions for the wide range of potential applications in device technology due to the presence of three different chemical components which allow, at least in principle, the tailoring of several important physical properties. The physics of these compounds spans many areas of fundamental and technological interest, such as magnetism and superconductivity [2,3]. Basic compounds of this family of materials are the chalcopyrites and the compounds with general chemical formula $A^{II}B_2^{III}C_4^{VI}$ or $A^{IV}B_2^{II}C_4^{VI}$ (so-called spinels), where the roman numerals indicate the appropriate column of the periodic table. Generally, when C=O or S, the spinel compounds crystallize in the cubic spinel structure. Spinels comprise an important class of ceramic compounds with a variety of interesting physical properties. Some of them are superconductors with relatively high transition temperatures [4]. Others have geophysical [5] and magnetism application [6,7]. Other ones are used as transparent conducting oxides in optoelectronic devices such as flat-panel displays and solar cells [8].

Among the ternary $A^{II}B_2^{III}C_4^{VI}$ compounds, the magnesium and cadmium indium sulfide XIn_2S_4 (X=Mg and Cd) crystallize in the cubic spinel structure. These compounds are currently used for

* Corresponding author at: Institute of Physical Biology, South Bohemia University, Nove Hrady 373 33, Czech Republic.
E-mail address: maalidph@yahoo.co.uk (A.H. Reshak).

0022-4596/$ - see front matter © 2010 Elsevier Inc. All rights reserved.
doi:10.1016/j.jssc.2010.09.022

optoelectronic application as photoconductors. They are also considered as promising candidate for intermediate-band (IB) formation because their band gaps lie in the region of optimum gaps for the implementation of an (IB) material [9]. These compounds have been known for a long time and have been the subject of many experimental and theoretical works. Many workers have succeeded in elaborating them by different techniques [10–19]. The optical properties such as photoluminescence, absorption, reflectivity, and Raman scattering have been reported by several authors [10,13,14,16–22]. The electronic properties have been investigated by several researchers [13,23–28]. $MgIn_2S_4$ has a band gap ranging from 2.1 to 2.28 eV. But the assumption that this band gap is direct or indirect is not obvious [25,29,30]. In the case of $CdIn_2S_4$, the direct band gap shows a wide range of values in the literature: it varies from 2.35 to 2.63 eV. Here, there is also some controversy on the nature of the band gap (direct or indirect) [10,12,24,25]. Till now, there are no reported theoretical or experimental data in the literature on the first order elastic constants and their pressure dependences for the compounds of interest. Moreover, there are no theoretical studies for the optical properties and the pressure dependence of band gaps of the investigated compounds. All the theoretical calculations devoted to these compounds are not full potential calculations. The reasons mentioned above motivate us to perform these calculations in order to provide another reference data for the existing theoretical works on this fascinating class of materials, using the full-potential (linear) augmented plane-wave plus local orbital (FP-(L)APW+lo) method within the density functional theory (DFT), which has proven to be one of the most accurate methods [31,32] for the computation of the electronic structure of solids.

The rest of the paper has been divided in three parts. In Section 2, we briefly describe the computational techniques used in this study. The most relevant results obtained for the structural, elastic, electronic, and optical properties for $MgIn_2S_4$ and $CdIn_2S_4$ compounds are presented and discussed in Section 3. Finally, in Section 4, we summarize the main conclusions of our work.

2. Computational method

The calculations were performed in the framework of the density functional theory (DFT). We have employed a full relativistic version of the full-potential linearized-augmented plane wave with the mixed basis FP/APW+lo method [33,34] as implemented in WIEN2K computer package [35]. The exchange-correlation contribution was described within the generalized gradient approximation (GGA) of Perdew–Burke–Ernzerhof (PBE) [36] to calculate the total energy, while for the electronic properties in addition to that the Engel–Vosko (EV-GGA) formalism [37] was also applied. In this method the space is divided into an interstitial region (IR) and non-overlapping muffin tin (MT) spheres centered at the atomic sites. In the IR region, the basis set consists of plane waves. Inside the MT spheres, the basis sets is described by radial solutions of the one particle Schrödinger equation (at fixed energy) and their energy derivatives multiplied by spherical harmonics. Spin–orbit coupling was included using the second variation method. The wave functions in the interstitial region were expanded in plane waves with a cut-off $K_{max}=12/R_{MT}$, where R_{MT} denotes the smallest atomic sphere radius and K_{max} is the maximum modulus for the reciprocal lattice vectors. The R_{MT} are taken to be 2.4, 2.8, 1.8, and 2.5 atomic units (au) for Mg, Cd, S, and In, respectively. The valence wave functions inside the spheres are expanded up to $l_{max}=9$, while the charge density was Fourier expanded up to $G_{max}=14\,(\mathrm{Ryd})^{1/2}$. The self-consistent calculations are considered to be converged when the total energy of the system is stable within 10^{-5} Ryd. The integrals over the Brillouin zone are performed up to 18 k-points in the irreducible Brillouin zone, using the Monkhorst–Pack special k-points approach [38].

3. Results and discussion

3.1. Structural and elastic properties

Cubic spinel compounds with general chemical formula AB_2X_4, where A and B are both cations while X is anion, have a closed packed face-centered-cubic structure, with space group $Fd-3m$ (#227), and their unit cell contains eight AB_2X_4 molecules. The 32 anions (X atoms) occupy the 32e site. The cations occupy either the tetrahedral 8a site (A atoms) or the octahedral 16d site (B atoms). There is only one internal parameter u, which specifies the deviation of the anions in the $\langle 111\rangle$ direction. The description of the atomic positions in spinels is dependent on the choice of setting for the origin in the $Fd-3m$ space group. Two different equipoints with point symmetries $-43m$ and $-3m$ are possible choices for the unit cell origin. In the ideal spinel with no anion deviation, $u_{ideal}=0.25$ or 0.375 for origins at $-3m$ or $-43m$ symmetry, respectively [39]. The X atoms are positioned at the (u, u, u) positions, the eight A atoms at (0.125, 0.125, 0.125), and the sixteen B atoms at (0.5, 0.5, 0.5). Then its crystal structure is characterized by two free parameters: the lattice constant a and the internal anion parameter u. In most spinels, u lies between 0.24 and 0.275, if the origin of the unit cell is taken at $-3m$ point symmetry. In our calculations, we have optimized the value of the internal parameter u by relaxing 'S' atomic positions inside the unit cell using the experimental lattice parameter. The optimized values of the internal parameter u are used to calculate the total energies for specified sets of lattice constants. The total energies versus unit cell volume are fitted to the Murnaghan's equation of state (EOS) [40] to determine the ground state properties such as the equilibrium lattice constant a_0, the bulk modulus B_0, and the bulk modulus pressure derivative B'. The calculated structural parameters of $MgIn_2S_4$ and $CdIn_2S_4$ are summarized in Table 1. Results from earlier experimental and theoretical works are quoted for comparison. Our computed values of the lattice constants for both compounds are slightly overestimated within 1.5% to the corresponding experimental values. This is attributed to our use of the generalized gradient approximation (GGA), which is known to overestimate the lattice constant value

Table 1
Lattice constant a_0 (in Å), sulfide free internal parameters u, and bulk modulus B_0 (in GPa) and its pressure derivative of the bulk modulus B' for $MgIn_2S_4$ and $CdIn_2S_4$. Experimental data are quoted for comparison.

	Present	Expt	Others
$MgIn_2S_4$			
a (Å)	10.917	10.7108[a]	10.523[b]
B (GPa)	66.53	55.42	79.00[b]
B'	4.95	4.95	
u	0.2565	0.258[a];0.257[c]	0.256[b]
$CdIn_2S_4$			
a (Å)	11.107	10.853[d]	
B (GPa)	66.90		
B'	5.17		
u	0.2616		

[a] Ref. [19].
[b] Ref. [26].
[c] Ref. [30].
[d] Ref. [14].

compared to the measured one. In order to show how the internal parameter u behave under pressure, the equilibrium geometries of the $MgIn_2S_4$ and $CdIn_2S_4$ unit cells were computed at fixed values of the applied hydrostatic pressure in the range from 0 to 12 GPa, with a step of 4 GPa, where at each pressure, a complete optimization of the internal parameter is performed. The pressure dependence of the internal parameter u is shown in Fig. 1. It is clearly seen that these compounds exhibit a negative u versus pressure slope, indicating that the spinel structure try to reach the ideal structure characterized by $u=0.25$ under pressure effect.

The elastic constants C_{ij} are fundamental and indispensable for describing the mechanical properties of materials. These constants determine the response of the crystal to the external forces. There are 21 independent elastic constants C_{ij}, but the symmetry of cubic crystal reduces this number to only three independent elastic constants C_{11}, C_{12}, and C_{44}. The bulk modulus B for cubic systems is expressed as a linear combination of C_{11} and C_{12}. The elastic constants C_{ij} are obtained by calculating the total energy as a function of volume conserving strains that break the symmetry. Further details of the calculation can be found elsewhere [41–43]. The present values of the elastic constants for $MgIn_2S_4$ and $CdIn_2S_4$ are given in Table 2. In view of Table 2, one can remark that the computed elastic constants values of $MgIn_2S_4$ are not very different from those of $CdIn_2S_4$. On the other side, it can be observed that the unidirectional elastic constant C_{11} is about 75% higher than C_{44}, so these compounds present a weaker resistance to the pure shear deformation compared to the resistance to the unidirectional compression.

A given crystal structure cannot exist in a stable or metastable phase unless its elastic constants obey certain relationship. The requirement of mechanical stability in a cubic structure leads to the following restrictions on the elastic constants [44]:

$$\frac{1}{3}(C_{11}+2C_{12})>0; \quad C_{44}>0; \quad \frac{1}{2}(C_{11}-C_{12})>0$$

These criteria are satisfied, indicating that these compounds are stable against elastic deformations.

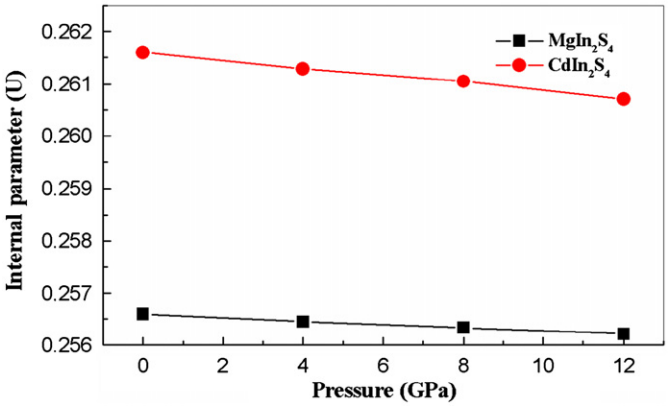

Fig. 1. Pressure dependence of the internal parameter u for $MgIn_2S_4$ and $CdIn_2S_4$.

The elastic anisotropy is an important factor, as it is highly correlated with possibility of inducing microcracks in the materials. For completely isotropic systems, the anisotropy factor A takes the value of the unity and the deviation from unity measures the degree of elastic anisotropy. The calculated values of the anisotropic factor A are found to be equal to 0.972 for $MgIn_2S_4$ and 0.81 for $CdIn_2S_4$, meaning that they are not characterized by a profound anisotropy.

The elastic constants C_{11}, C_{12}, and C_{44} are estimated from first-principles calculations for $MgIn_2S_4$ and $CdIn_2S_4$ single-crystals. However, the prepared materials are in general polycrystalline, and therefore it is important to evaluate the corresponding moduli for the polycrystalline species. Using the Voigt–Reus–Hill approximations [45,46], some polycrystalline elastic moduli, namely, the shear modulus G, the Young's modulus E, and the Poisson's ratio ν, have been calculated from the single-crystal elastic constants C_{ij}. The calculated values of the mentioned elastic moduli for polycrystalline $MgIn_2S_4$ and $CdIn_2S_4$ aggregates are listed in Table 2. Having acquired the necessary data, we now try to elaborate more on the ductile or brittle nature of these compounds. The ductility and brittleness behaviors of materials can be explained from some proposed relationship. Pugh [47] has proposed a simple relationship that links empirically the plastic properties of materials with their elastic moduli by B/G. The critical value which separates ductile and brittle materials is around 1.75; if $B/G>1.75$, the material behaves in a ductile manner; otherwise the material behaves in a brittle manner. The values for Pugh's criterion B/G ratio are found to be equal 2.52 for $MgIn_2S_4$ and 2.85 for $CdIn_2S_4$. These values are higher than the critical value (1.75), which clearly highlights the ductile nature of both compounds. Another index of the brittle–ductile characteristic of the materials is the Cauchy's pressure, defined as the difference between the elastic constants $C_{11}-C_{12}$. If the Cauchy's pressure is positive (negative), the material is expected to be ductile (brittle) [48,49]. Here, the calculated Cauchy's pressure is positive for both compounds. Therefore, these compounds are classified as ductile materials.

Having calculated the Young's modulus E, the bulk modulus B, and the shear modulus G, one can calculate the Debye temperature θ_D, which is an important fundamental parameter closely related to many physical properties such as elastic constants, specific heat, and melting temperature. One of the standard methods to calculate the Debye temperature (θ_D) is from the elastic constants data, using the classical relation [50]. The average, longitudinal, and transversal sound velocities are obtained using relations given in Refs. [34,51]. The calculated values of sound velocity and Debye temperature as well as the density for $MgIn_2S_4$ and $CdIn_2S_4$ are those given in Table 3. In view of Table 3, we can remark that the Debye temperature decreases when going from $MgIn_2S_4$ to $CdIn_2S_4$. To the best of our knowledge, there are no experimental or theoretical data for elastic constants of $MgIn_2S_4$ and $CdIn_2S_4$ compounds given in the literature. Then, our results can serve as a prediction for future investigations.

In the following paragraph we shed more light on the pressure dependence of the elastic properties. Fig. 2 shows the variation of

Table 2
Calculated single-crystal elastic constants (C_{11}, C_{12}, and C_{44}, in GPa) and polycrystalline elastic parameters (shear modulus G (in GPa), Young's modulus E (in GPa), and Poisson's ratios σ) for $MgIn_2S_4$ and $CdIn_2S_4$.

System	C_{11}	C_{12}	C_{44}	E	G	σ
$MgIn_2S_4$	102.34	48.62	26.11	69.96	26.40	0.32
$CdIn_2S_4$	102.46	49.13	21.46	62.89	23.41	0.34

Table 3
Calculated density (ρ, in g/cm^3), longitudinal, transverse, and average sound velocity (v_l, v_t, and v_m, in m/s) and Debye temperature (θ_D, in K) for $MgIn_2S_4$ and $CdIn_2S_4$ compounds.

System	ρ	v_l	v_t	v_m	θ_D
$MgIn_2S_4$	3.90	5105.9	2601.3	3469.5	362.0
$CdIn_2S_4$	4.56	4638.8	2265.8	3047.5	312.5

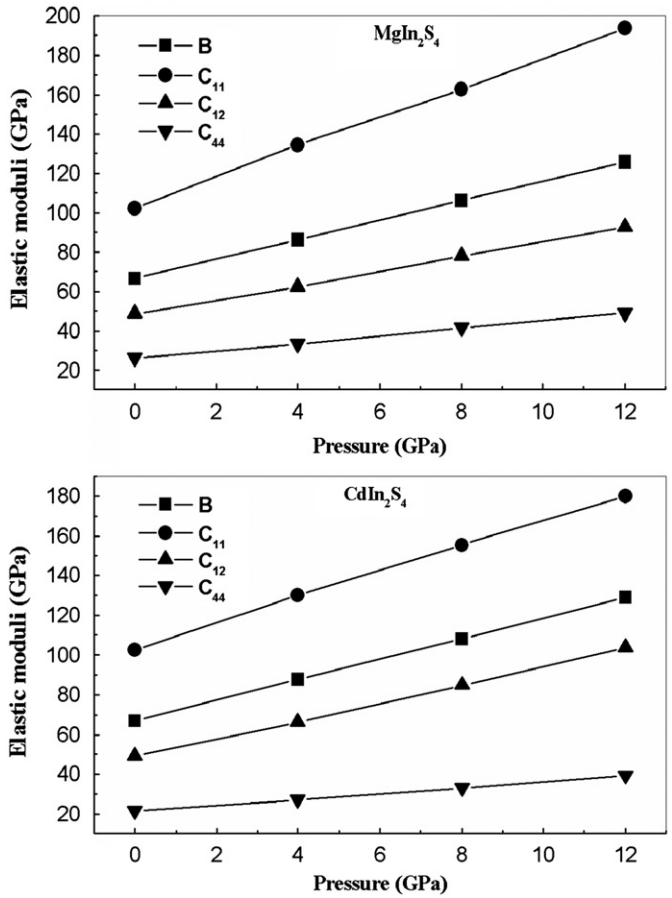

Fig. 2. Pressure dependence of the elastic constants (C_{11}, C_{12}, and C_{44}) and the bulk modulus B for $MgIn_2S_4$ and $CdIn_2S_4$.

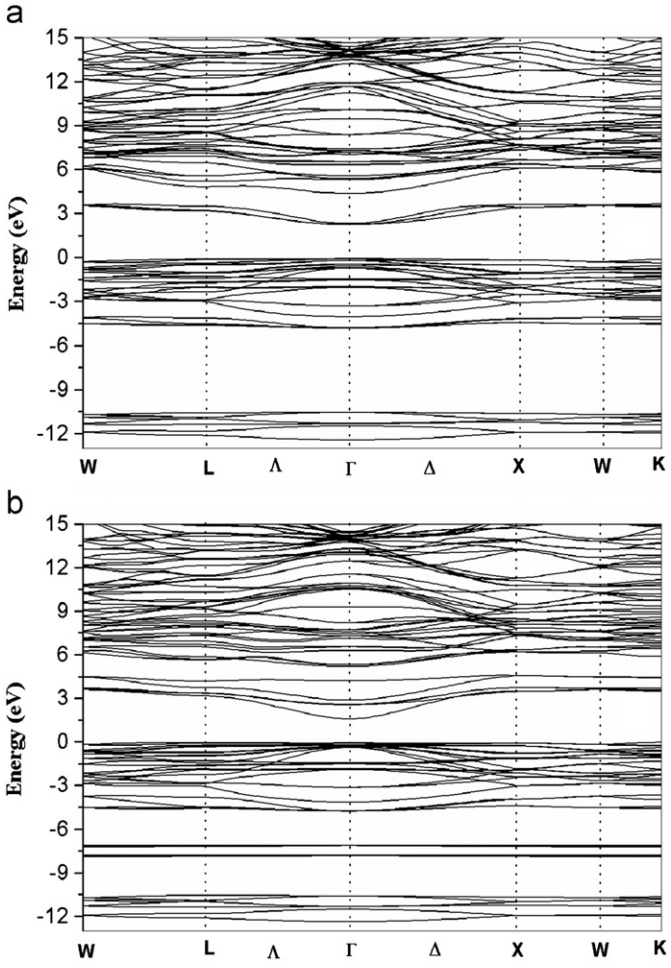

Fig. 3. EV-GGA electronic band dispersion curves of $MgIn_2S_4$ (a) and $CdIn_2S_4$ (b) along some high symmetry directions of the Brillouin zone.

Table 4
Calculated pressure derivatives of the elastic constants and bulk modulus for $MgIn_2S_4$ and $CdIn_2S_4$.

System	$\frac{\partial B_0}{\partial P}$	$\frac{\partial C_{11}}{\partial P}$	$\frac{\partial C_{12}}{\partial P}$	$\frac{\partial C_{44}}{\partial P}$
$MgIn_2S_4$	4.95	7.55	3.67	1.92
$CdIn_2S_4$	5.17	6.42	4.54	1.48

the elastic constants (C_{11}, C_{12}, and C_{44}) and the bulk modulus (B) of $MgIn_2S_4$ and $CdIn_2S_4$ as a function of pressure. We clearly predict that the elastic constants C_{11}, C_{12}, and C_{44} increase when the pressure is enhanced. A linear pressure dependence of C_{11}, C_{12}, C_{44}, and B curves is found. The pressure coefficients of the elastic constants and bulk modulus are determined by least-square linear fits. The calculated linear pressure coefficients are listed in Table 4. It is clear that the C_{11} is more sensitive to the change of pressure compared to the other elastic modulus. C_{44} is less sensitive to the change of pressure.

3.2. Band structure and density of states

Now we turn our attention to study the electronic properties of $MgIn_2S_4$ and $CdIn_2S_4$ via calculating the energy band structure and density of states. Fig. 3 shows the calculated band structure at equilibrium volume within EV-GGA as a prototype since the band profiles are quite similar for both GGA and EV-GGA with a small difference in details. The valence band maximum (VBM) is located at the Γ point for $MgIn_2S_4$ and at the K point for $CdIn_2S_4$. The conduction band minimum (CBM) occurs at the Γ point in both compounds, resulting in a direct band gap at the Γ point for $MgIn_2S_4$ and an indirect band gap (K→Γ) for $CdIn_2S_4$.

To further elucidate the nature of the electronic band structure, we have also calculated the total and atomic site-projected *l*-decomposed densities of states (TDOS and PDOS) for these compounds. These are displayed in Fig. 4. From the partial PDOS we are able to identify the angular momentum character of the different structures. Starting from the lower energy side, the two deep electronic localized structures centered at around −14.19 and −13.51 eV below the Fermi level arises mainly from In-*d* states with a small admixture of S-*s* states. The second structure located at −12.0 eV originates from S-*s* states. In the case of $CdIn_2S_4$, the TDOS showed an additional structure localized at −7.5 eV. This structure consists mainly of Cd-*d* states. The upside of the valence band consists of S-*p* states. The structure at the lower part of the upper valence bands, between −4.0 and −5.0 eV, for both compounds originates from a mixture of In-*s* and S-*p* states. Continuing upward in energy, it is clear from Figs. 3 and 4 that the two studied compounds are semiconductors. In the conduction band, the structure from +2 to +4 eV which forms the lower part of the conduction bands is mainly In-*s* states hybridized with S-*p* states in $MgIn_2S_4$ and In/Cd-*s* states hybridized with S-*p* states in $CdIn_2S_4$. The high lying structure in the conduction bands (above +6.0 eV) is mixture of Mg/Cd/In/S-*p* states.

The calculated band gap values for $MgIn_2S_4$ and $CdIn_2S_4$ compounds within the GGA and EV-GGA are listed in Table 5,

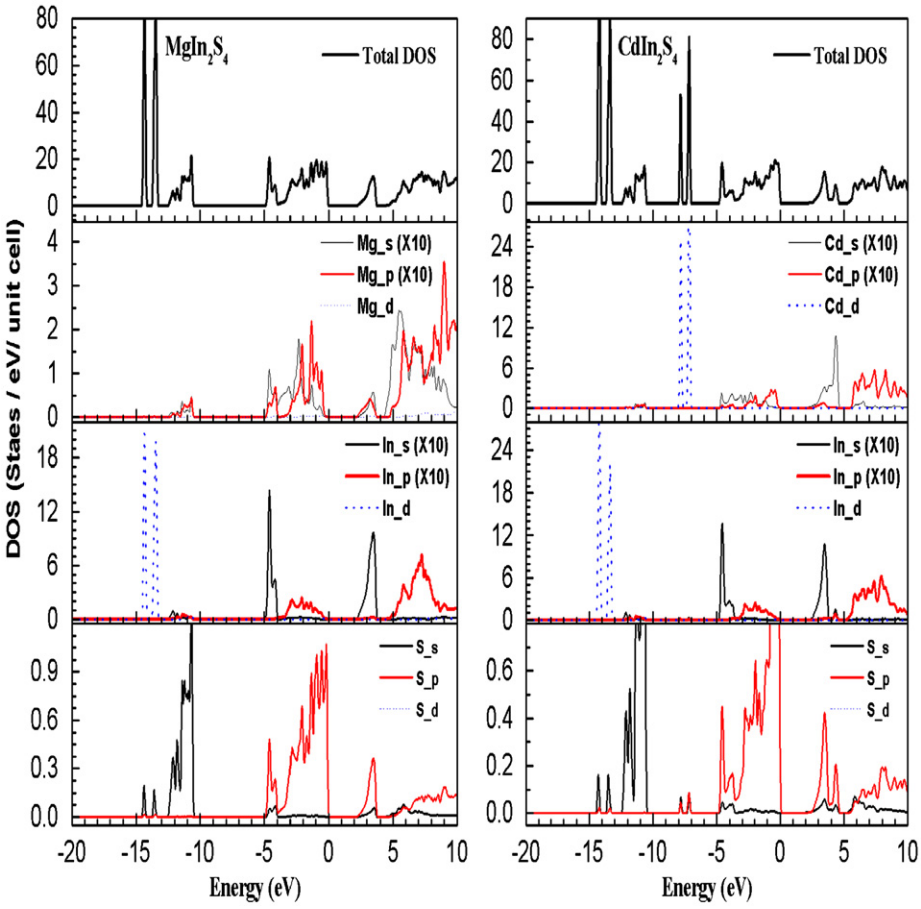

Fig. 4. Calculated total and partial densities of states for $MgIn_2S_4$ and $CdIn_2S_4$.

Table 5
Calculated direct (Γ–Γ and X–X) and indirect (K–Γ and K–X) band gaps for $MgIn_2S_4$ and $CdIn_2S_4$. All energies are in eV.

	Γ–Γ	X–X	K–Γ	K–X
$MgIn_2S_4$				
EVGGA	2.24	3.60	2.43	3.55
GGA	1.77	3.57	1.84	3.55
PP[a]	~2.40			
Expt[b]	2.28			
$CdIn_2S_4$				
EVGGA	1.92	3.80	1.77	3.48
GGA	1.12	3.22	1.07	3.15
PP[c]	~2.75		2.2	
Expt[d]	2.35			
Expt[e]	2.70			

[a] Ref. [26].
[b] Ref. [30].
[c] Ref. [24].
[d] Ref. [15].
[e] Ref. [13].

along with the experimental values and other previous theoretical calculations. It is clearly seen that the band gaps predicted by GGA are lower than the experiment values. This well-known underestimation of the band gap is mainly due to the fact that the simple form of GGA is not sufficiently flexible for accurately reproduce both exchange-correlation energy and its charge derivative. Engel and Vosko [37] constructed a new functional form of the GGA, namely, EV-GGA, which proved to improve the results for quantities that depend on the energy eigenvalues, including the band gaps [52]. The values of the calculated band gaps with EV-GGA show a significant improvement over the results based on GGA compared to the experimental value.

Knowledge of the electron and hole effective mass values is indispensable for the understanding of transport phenomena, exciton effects, and electro-hole in semiconductors. Excitonic properties are of great interest for $MgIn_2S_4$ and $CdIn_2S_4$; therefore, it is worthwhile to estimate the electron and hole effective mass values for these materials. Experimentally, the effective masses are usually determined by cyclotron resonance, electroreflectance measurements or from analysis of transport data or transport measurements [53]. Theoretically, the effective masses can be estimated from the energy band curvatures. Generally, the effective mass is a tensor with nine components; however, for the much idealized simple case, where the E–k diagram can be fitted by a parabola $E=\hbar^2k^2/2m^*$, the effective mass becomes a scalar at high symmetry point in Brillouin zone. We have computed the electron effective mass at the conduction band minima (CBM) and the hole effective mass at the valence band maxima (VBM) for $MgIn_2S_4$ and $CdIn_2S_4$. The electron effective mass value is obtained from the curvature of the energy band near the Γ-point at the CBM for both compounds. The hole effective masse value is calculated from the curvature near the Γ-point at the VBM for $MgIn_2S_4$, and near the K point at the VBM for $CdIn_2S_4$. The calculated electron and hole effective mass values for $MgIn_2S_4$ and $CdIn_2S_4$ are shown in Table 6. The electron and hole effective masses are quite isotropic for the spinel compounds. We find that the effective mass of $MgIn_2S_4$ is larger than that of $CdIn_2S_4$, due to the higher band gap of $MgIn_2S_4$. As a small effective mass yields a

Table 6
Electron (m_e^*), heavy hole (m_{hh}^*) and light hole (m_{lh}^*) effective masses (in units of free electron mass m_0) for $MgIn_2S_4$ and $CdIn_2S_4$.

m_e^*	m_{hh}^*	m_{lh}^*	
$MgIn_2S_4$	0.4902	0.8607	0.7297
$CdIn_2S_4$	0.17318	0.6148	//

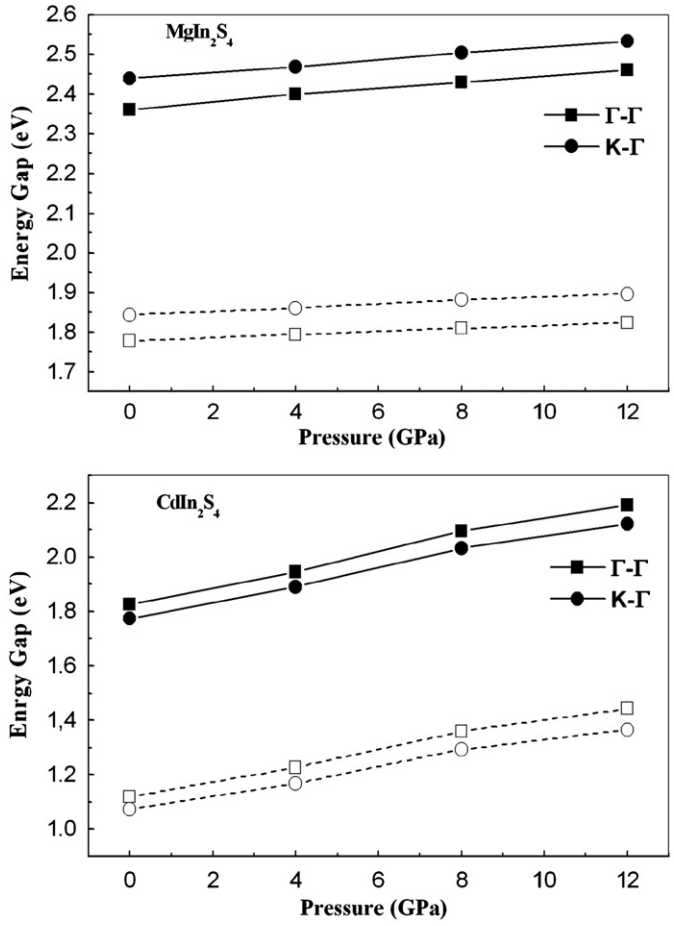

Fig. 5. Calculated energy band gaps direct ($\Gamma \rightarrow \Gamma$) and indirect ($K \rightarrow \Gamma$) of $MgIn_2S_4$ and $CdIn_2S_4$ versus pressure, within GGA (dotted line) and EV-GGA (solid line).

high conductivity, therefore, the conductivity should be larger in $CdIn_2S_4$. From Table 6 data, we can outline that holes are much heavier than electrons, especially in $CdIn_2S_4$, so carrier transport in these compounds should be dominated by electrons.

In order to investigate the effect of the pressure on the size of the energy gaps of $MgIn_2S_4$ and $CdIn_2S_4$ compounds, the band energies at selected symmetry points are examined as a function of pressure. Fig. 5 shows the plots of the pressure variation of the direct gap ($\Gamma-\Gamma$) and indirect gap ($K-\Gamma$) for the two studied compounds within GGA and EV-GGA. Fig. 5 shows that ($\Gamma-\Gamma$) and ($K-\Gamma$) band gaps increase with increase in the pressure with the same propensity. The EV-GGA (GGA) calculated band gap linear pressure coefficients, $dE_{\Gamma-\Gamma}/dp$ and $dE_{K-\Gamma}/dp$, are found to be equal to 15 (12) and 7 (5), respectively, for $MgIn_2S_4$. For $CdIn_2S_4$, $dE_{\Gamma-\Gamma}/dp$ and $dE_{K-\Gamma}/dp$ are equal to 53 (45) and 34 (28) meV$(GPa)^{-1}$, respectively. Our calculated EV-GGA band gap linear pressure coefficients along the (Γ–Γ) direction are in good agreement with the measured ones, which are 20.0 meV $(GPa)^{-1}$ for $MgIn_2S_4$ and 70 meV $(GPa)^{-1}$ for $CdIn_2S_4$ [10].

3.3. Optical properties

The optical properties of matter can be described by the complex dielectric function $\varepsilon(\omega)$, which represents the linear response of a system to an external electromagnetic field. It can be expressed as $\varepsilon(\omega)=\varepsilon_1(\omega)+i\varepsilon_2(\omega)$, where $\varepsilon_1(\omega)$ and $\varepsilon_2(\omega)$ are the real and imaginary components of the dielectric function, respectively. Generally, there are two contributions to $\varepsilon(\omega)$, namely, intraband and interband transitions. The contribution from intraband transitions is crucial only for metals. The interband transitions can further be split into direct and indirect transitions. Here we ignore the indirect interband transitions which involve scattering of phonon and are expressed to give only a small contributions to $\varepsilon(\omega)$. The imaginary part $\varepsilon_2(\omega)$ is directly related to the electronic band structure and it can be computed by summing up all possible transitions from the occupied to the unoccupied states, taking into account the appropriate transition dipole matrix elements. A full detail description of the calculation of these matrix elements is given by Ambrosch-Draxl and Sofo [54]. The real part $\varepsilon_1(\omega)$ can be derived from the imaginary part using the familiar Kramers–Kronig transformation. The knowledge of both real and imaginary parts of the dielectric function allows the calculation of various optical constants, such as the spectral reflectivity $R(\omega)$, the refractive index $n(\omega)$, and the electron energy loss function $L(\omega)$ using standard expressions [55,56].

In the calculations of the optical properties, a dense mesh of uniformly distributed k-points is required. Hence, the Brillouin zone integration was performed with 286 k-points in the irreducible part of the Brillouin zone (IBZ). Broadening is taken to be 0.15 eV. The EV-GGA was used to perform optical properties calculations since it yields better band gaps than GGA.

Fig. 6 displays the calculated real and imaginary parts of the dielectric function at zero pressure and at 30 GPa for $MgIn_2S_4$ and $CdIn_2S_4$. The inset shows the measured real and imaginary parts spectra for $CdIn_2S_4$ by Grilli and co-workers [13] at 300 K. As it can be seen, the $\varepsilon_2(\omega)$ spectrum does not vary greatly from $MgIn_2S_4$ to $MgIn_2S_4$. This is attributed to the fact that the conduction bands features and the symmetries of the wave functions, which dictate the selection rules and are fully reflected in the Matrix Moment Elements, are somewhat similar. The calculated $\varepsilon_2(\omega)$ spectra show that the first critical points occur at about 2.52 and 1.64 eV for $MgIn_2S_4$ and $CdIn_2S_4$, respectively. These points are $\Gamma_V-\Gamma_C$ splitting, which gives the threshold for direct optical transitions between the sulphide 'p' valence band maximum and the first conduction band minimum. This is known as the fundamental absorption edge. The critical points are followed by two structures. The first one situated at about 4.46 eV in both compounds is related to the direct transitions between the higher valence band and the fifth conduction band along W–L and Δ directions. Our result on the location of this structure for $CdIn_2S_4$ is in disagreement with the reflectivity measurement. The second structure is localized at about 6.10 and 6.21 eV for $MgIn_2S_4$ and $CdIn_2S_4$, respectively. It seems not realistic to interpret the origin of the above mentioned energy-peaks in the optical spectra since many transitions (direct and indirect) are taking place at the corresponding energy in the band structure. When these materials are compressed the positions of all critical points cited above are shifted with an enhanced energy compared to that at zero pressure. The reason lies on the enhancement of direct and indirect gaps under pressure effect. Although their positions are shifted under pressure, these points still have the same type as that at zero pressure with increase in the intensity of the second and third peaks.

The refractive index $n(\omega)$, the reflectivity $R(\omega)$, and the electron energy loss spectra $L(\omega)$ for $MgIn_2S_4$ and $CdIn_2S_4$

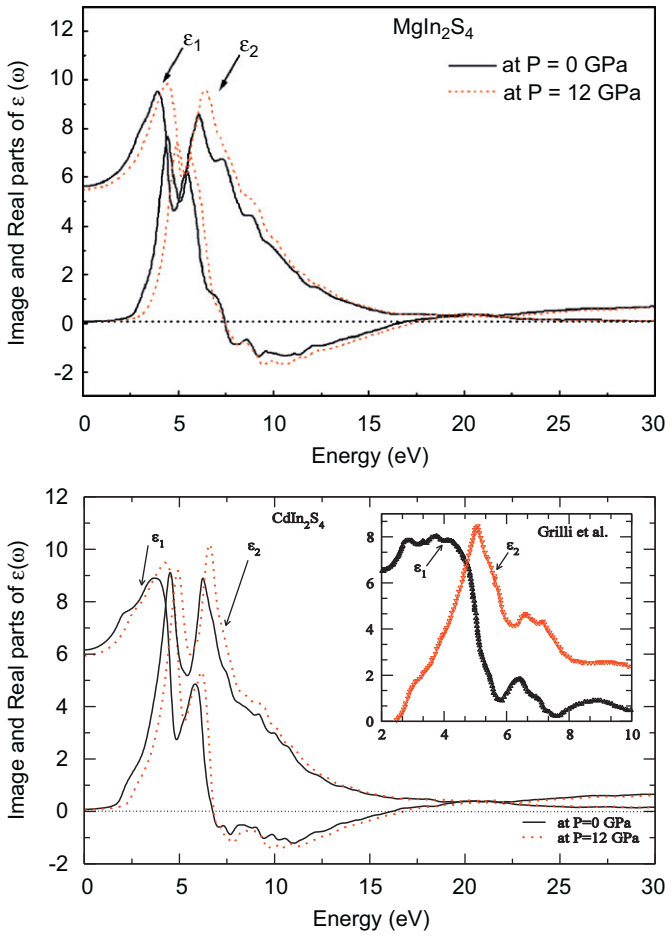

Fig. 6. Calculated EV-GGA-real and imaginary parts of the dielectric function for $MgIn_2S_4$ and $CdIn_2S_4$: at zero pressure (solid line) and at $P=12$ GPa (dotted line).

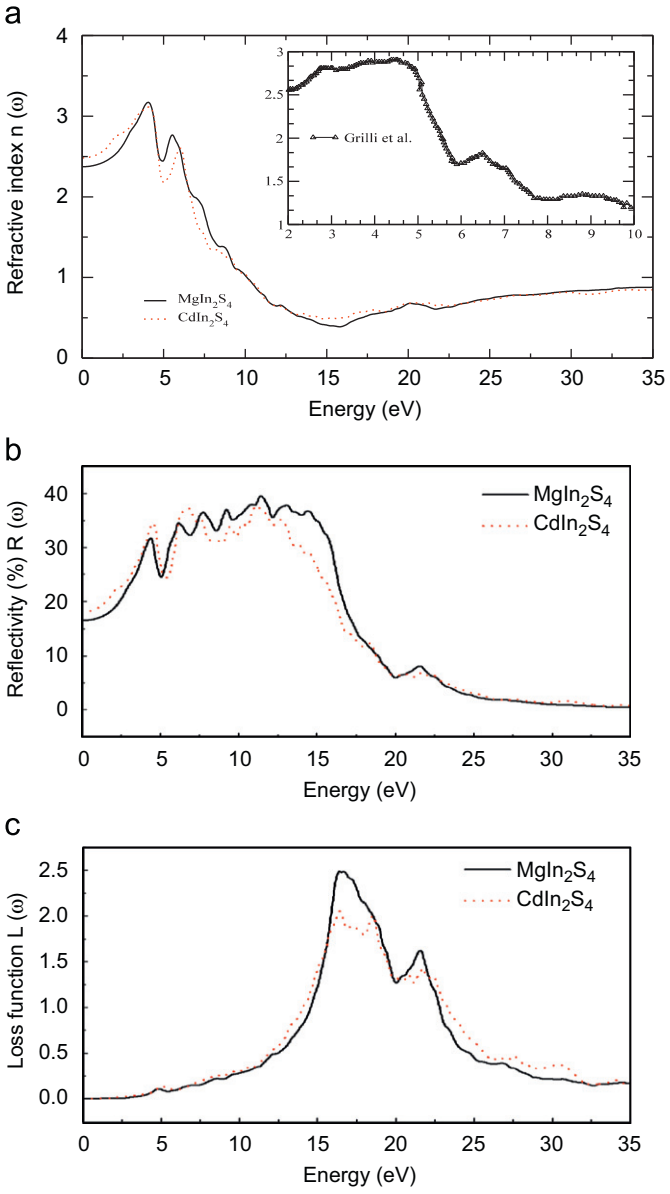

Fig. 7. Calculated refractive index $n(\omega)$, reflectivity $R(\omega)$, and electron energy loss $L(\omega)$ spectra for $MgIn_2S_4$ (solid line) and $CdIn_2S_4$ (dotted line).

compounds are displayed in Fig. 7. The experimental refractive index $n(\omega)$ spectrum for $CdIn_2S_4$ is also presented in the inset of Fig. 7(a). The overall profile of $n(\omega)$, $R(\omega)$, and $L(\omega)$ spectra is similar in the two studied compounds except that there is an energy shift at the energies ranging from 0.0 to 10.2 eV for $n(\omega)$ and $R(\omega)$ spectra. The refractive index reaches a maximum value of 3.2 at 3.17 eV for both compounds. From the reflectivity spectra of these compounds, we note that $R(\omega)$ increases up to about 40.2% and then starts to decrease at around 13.8 eV. The plot of the energy loss function $L(\omega)$ shows a wider peak situated at about 16.50 eV for the two compounds. This peak defines the screened plasma frequency ω_p [57], and corresponds to the abrupt reduction of the reflectivity spectrum $R(\omega)$ and to the zero crossing of $\varepsilon_1(\omega)$.

The static dielectric constant $\varepsilon_1(0)$ is given by the low energy limit of $\varepsilon_1(\omega)$. It is necessary to emphasize that we do not include phonon contributions to the dielectric screening, and $\varepsilon_1(0)$ corresponds to the static optical dielectric constant. The static optical dielectric constants obtained in this way are 5.64 and 6.20 for $MgIn_2S_4$ and $CdIn_2S_4$, respectively. Our calculated static optical dielectric constant for $CdIn_2S_4$ is slightly underestimated than the experimental results (≈ 6.76) [13]. Fig. 8 shows the pressure dependence of the dielectric constant $\varepsilon(0)$ for the investigated compounds within EV-GGA formalism. As it can be seen, the decrease of the static dielectric constant (static refractive index) with pressure is practically linear. The pressure derivatives of the refractive index n of these compounds are determined by a linear fit. The calculated pressure $(1/n_0)(dn/dp)$ for $MgIn_2S_4$ and $CdIn_2S_4$

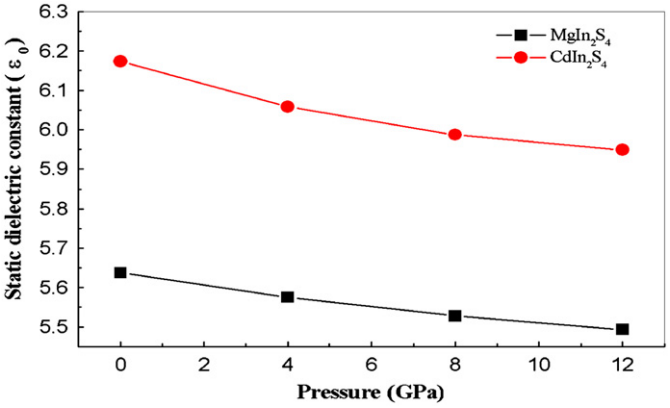

Fig. 8. Pressure dependence of the static optical dielectric constant $\varepsilon(0)$ for $MgIn_2S_4$ and $CdIn_2S_4$ within EV-GGA.

are found to be equal to -1.06×10^{-2} and $-1.52\times10^{-2}\,GPa^{-1}$, respectively.

4. Conclusions

We have performed detailed investigation on the structural, elastic, electronic, and optical properties of spinel magnesium and cadmium indium sulfides $MgIn_2S_4$ and $CdIn_2S_4$ using first-principles FP-APW+lo method within GGA and EV-GGA. The calculated ground-state properties such as lattice constant, bulk modulus, and internal free parameter agree well with the available experimental data. The elastic constants, which have not yet been calculated or measured, were obtained using the volume conserving strain technique. A linear dependence of the bulk modulus and elastic constants versus the applied pressure is found. Polycrystalline elastic moduli, namely, Shear modulus, Young's modulus, Poisson's ratio, sound velocities, and Debye temperature were derived from the obtained single-crystal elastic constants. From these results, both compounds are classified as ductile materials. Our results for the band structure and DOS show that both compounds are semiconductors with a direct band gap (Γ–Γ) for $MgIn_2S_4$ and an indirect band gap (K–Γ) for $CdIn_2S_4$. Results obtained for energy band gaps using EV-GGA show a significant improvement over the GGA calculations. Our calculated pressure-induced energy shifts for both compounds along the (Γ–Γ) direction are comparable to the experimental data. The imaginary and real parts of the dielectric function at ambient and at 12 GPa pressure were investigated and analyzed to identify the optical transitions. The static dielectric constants $\varepsilon(0)$, static refractive index $n(0)$, and the pressure coefficients of $n(0)$ have been calculated.

Acknowledgement

For the author Ali Hussain Reshak this work was supported from the institutional research concept of the Institute of Physical Biology, UFB (No. MSM6007665808), the program RDI of the Czech Republic, the Project CENAKVA (No. CZ.1.05/2.1.00/01.0024), the Grant no. 152/2010/Z of the Grant Agency of the University of South Bohemia and the School of Microelectronic Engineering, University Malaysia Perlis (UniMAP), Block A, Kompleks Pusat Pengajian, 02600 Arau Jejawi, Perlis, Malaysia.

References

[1] M.I. Eremets, K. Shimizu, K. Amaya, Science 281 (1998) 1333.
[2] S.K. Deb, A. Zunger (Eds.), Proceeding of Seventh International Conference on Ternary and Multinary Compounds, MRSPittsbourg, 1987.
[3] S. Lundqvist, E. Tosatti, M.P. Tosi, Y. Lu (Eds.), Proceeding of the Adriaico Research Conferences on High Temperatures Superconductor, World Scientific, Singapore, 1987.
[4] R.W. McCallum, D.C. Johnston, C.A. Luengo, M.B. Maple, J. Low Temp. Phys. 25 (1976) 177.
[5] T. Irifune, K. Fujino, E. Ohtani, Nature (London) 349 (1991) 409.
[6] H. Martinho, N.O. Monero, J.A. Sanjuro, C. Rottori, A.J. Garia-Adeva, D.L. Huber, S.B. Oseroff, W. Ratcliff, S.W. Cheong, P.G. Pagliuso, J.L. Sarrao, G.B. Martin, Phys. Rev. B 64 (2001) 024408.
[7] R. Masrour, J. Alloys Compd. 489 (2010) 441.
[8] D. Sagev, S.-H. Wei, Phys. Rev. B 71 (2005) 125129.
[9] A. Luque, A. Marti, Phys. Rev. Lett. 78 (1997))5014.
[10] J. Ruiz-Fuertes, D. Errandonea, F.J. Manjón, D. Martinez-Garcia, A. Segura, V.V. Ursaki, I.M. Tiginyanu, J. Appl. Phys. 103 (2008) 063710.
[11] H. Hahn, W. Klingler, Z. Anorg. Allg. 263 (1950) 177.
[12] H. Nakanishi, S. Eudo, T. Trie, Jpn. J. Appl. Phys. 12 (1973) 1646.
[13] E. Grilli, M. Guzzi, A. Anedda, F. Raga, A. Serpi, Solid State Commun. 27 (1978) 105.
[14] T. Takizawa, H. Ohwada, H. Kobayashi, K. Kanbara, T. Irie, S. Endo, H. Nakanishi, H. Kato, H. Fukutani, Solid State Commun. 67 (1988) 739.
[15] M.M. El-Nahass, Appl. Phys. A 52 (1991) 353.
[16] E. Fortin, S. Fafard, A. Anedda, F. Ledda, A. Charlebois, Solid State Commun. 77 (1991) 165.
[17] A.V. Kokate, M.R. Asabe, S.B. Shelake, P.P. Hankare, B.K. Chougule, Physica B 390 (2007) 84.
[18] S. Endo, T. Irie, J. Phys. Chem. Solids 37 (1976) 201.
[19] L. Gastaldi, A. Lapiccirella, J. Solid State Chem. 30 (1979) 223.
[20] N.N. Syrbu, M. Bogdanash, N.A. Moldovyan, Infrared Phys. Technol. 37 (1996) 763.
[21] V.V. Ursaki, F.J. Monjón, I.M. Tiginyanu, V.E. Tezlevan, J. Phys.: Condens. Matter 14 (2002) 6801.
[22] A. Anedda, E. Fortin, J. Phys. Chem. Solids 40 (1979))653.
[23] A.N. Gusatinskii, A.A. Lavrentyev, M.A. Blokhin, V.Yu. Slivka, Solis State Commun. 57 (1986) 389.
[24] F. Meloni, G. Mula, Phys. Rev. B 2 (1970) 393.
[25] S. Katsuki, Solid State Commun. 39 (1981) 767.
[26] M. Marineli, S. Baroni, F. Meloni, Phys. Rev. B 38 (1988) 8258.
[27] F. Cerrina, C. Quaresima, I. Abbati, L. Braicovish, P. Picco, G. Margaritendo, Solid State Commun. 33 (1980) 429.
[28] I. Aguilerea, P. Palacios, K. Sanchez, P. Wahnon, Phys. Rev. B 81 (2010) 075206.
[29] P.M. Sirimane, N. Soyonama, T. Takata, J. Solid State Chem. 154 (2000) 476.
[30] M. Wakaki, O. Shintani, T. Ogawa, T. Arai, Jpn, J. Appl. Phys 19 (Suppl. 19-3) (1980) 255.
[31] S. Gao, Comput. Phys. Commun. 153 (2003) 190.
[32] K. Schwarz, J. Solid State Chem. 176 (2003) 319.
[33] G.K.H. Madsen, P. Blaha, K. Schwarz, E. Sjöstedt, L. Nordström, Phys. Rev. B 64 (2001) 195134.
[34] K. Schwarz, P. Blaha, G.K.H. Madsen, Comput. Phys. Commun. 147 (2002) 71.
[35] P. Blaha, K. Schwarz, G.K.H. Madsen, D. Kvasnicka, J. Luitz, WIEN2k, An Augmented Plane Wave Plus Local Orbitals Program for Calculating Crystal Properties, Vienna University of Technology, Austria, 2001.
[36] J.P. Perdew, S. Burke, M. Ernzerhof, Phys. Rev. Lett. 77 (1996) 3865.
[37] E. Engel, S.H. Vosko, Phys. Rev. B 47 (1993) 13164.
[38] H.J. Monkhorst, J.D. Pack, Phys. Rev. B 13 (1976) 5188.
[39] S.M. Hosseini, Phys. Status Solidi (b) 245 (2008) 2800.
[40] F.D. Murnaghan, Proc. Natl. Acad. Sci. USA 30 (1944) 244.
[41] M.J. Mehl, Phys. Rev. B 47 (1993) 2493.
[42] R. Khenata, A. Bouhemadou, A.H. Reshak, R. Ahmed, B. Bouhafs, D. Rached, Y. Al Douri, M. Rérat, Phys. Rev. B 75 (2007) 195131.
[43] V. Kanchana, G. Vaitheeswaran, A. Svane, J. Alloys Compd. 455 (2008) 480.
[44] J. Wang, S. Yip, S.R. Phillpot, D. Wolf, Phys. Rev. Lett. 71 (1993) 4182.
[45] W. Voigt, in: Lehrbush der Kristallphysik, Taubner, Leipzig, 1928.
[46] E. Schreiber, O.L. Anderson, N. Soga, in: Elastic Constants and Their Measurement, McGraw-Hill, New York, 1973.
[47] S.F. Pugh, Philos. Mag. 45 (1954) 823.
[48] V. Kanchana, G. Vaitheeswaran, Yanning Ma, A. Yu Xie, O. Svane, Eriksson, Phys. Rev. B 80 (2009) 125108.
[49] M. Rajagopalan, S. Praveen Kumar, R. Anuthama, Physica B 405 (2010) 1817.
[50] O.L. Anderson, J. Phys. Chem. Solids 24 (1963) 909.
[51] W. Feng, S. Cui, H. Hu, G. Zhang, Z. Lv, Z. Gong, Physica B 405 (2010) 2599.
[52] P. Dufek, P. Blaha, K. Schwarz, Phys. Rev. B 50 (1994) 7279.
[53] O. Zakharov, A. Rubio, X. Blase, M.L. Cohen, S.G. Louie, Phys. Rev. B 50 (1994) 10780.
[54] C. Ambrosch-Draxl, J.O. Sofo, Comput. Phys. Commun. 175 (2006) 1.
[55] A. Delin, A.O. Eriksson, R. Ahuja, B. Johansson, M.S.S. Brooks, T. Gasche, S. Auluck, J.M. Wills, Phys. Rev. B 54 (1996) 1673.
[56] Y.P. Yu, M. Cardona, Fundamental of Semiconductors Physics and Materials Properties, second ed., Springer-Verlag, Berlin, 1999, p. 233.
[57] M. Fox, Optical Properties of Solids, Academic Press, New York, 1972.